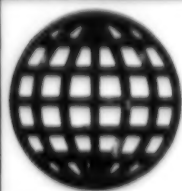


JPRS-UMS-92-008  
4 JUNE 1992



FOREIGN  
BROADCAST  
INFORMATION  
SERVICE

---

# ***JPRS Report***

# **Science & Technology**

---

***Central Eurasia:  
Materials Science***

# Science & Technology

## Central Eurasia: Materials Science

JPRS-UMS-92-008

### CONTENTS

4 June 1992

#### Analysis, Testing

Static and Cyclical Strength and Crack Resistance Characteristics of Welded Structural Steel Joints at Low Temperatures. Report 1 [V.V. Larionov, Kh.M. Khanukhov, et al.; PROBLEMY POCHNOSTI, No 2 (272), Feb 92]	1
Static and Cyclical Strength and Crack Resistance Characteristics of Welded Structural Steel Joints at Low Temperatures. Report 2 [V.V. Larionov, Kh.M. Khanukhov, et al.; PROBLEMY POCHNOSTI, No 2 (272), Feb 92]	1
Long-Term Strength of Welded Pipeline T-Joints [R.Z. Shron, E.I. Getsfrid, et al.; PROBLEMY POCHNOSTI, No 2 (272), Feb 92]	1
Method of Measuring Equivalent Stresses in Aircraft Gas Turbine Engine Blades [V.V. Malygin (deceased), D.F. Fedorchenko, et al.; PROBLEMY POCHNOSTI, No 2 (272), Feb 92]	1
Effect of Heat Treatment on Hydrogen Embrittlement Resistance of Age Hardenable Nickel Alloy [K.A. Yushchenko, V.S. Savchenko, et al.; METALLOVEDENIYE I TERMICHESKAYA OBRABOTKA METALLOV, No 1, Jan 92]	2
Structure and Properties of Titanium Alloys With Nitrogen [B.Ye. Paton, B.I. Medovar, et al.; METALLOVEDENIYE I TERMICHESKAYA OBRABOTKA METALLOV, No 1, Jan 92]	2

#### Coatings

Recrystallization of Multilayer CoNi/Cr Films [G.N. Kadykova, T.K. Lyakhovich, et al.; METALLOVEDENIYE I TERMICHESKAYA OBRABOTKA METALLOV, No 1, Jan 92]	3
---	---

#### Ferrous Metals

Relative Error of Measuring Oxygen Activity in Liquid Steel by Electrochemical Transducers [I.V. Zinkovskiy, Yu.I. Nebosov, et al.; IZVESTIYA VYSSHIKH UCHEBNYKH ZAVEDENIY: CHERNAYA METALLURGIYA, No 1, Jan 92]	4
Improved Heat Balance Analysis Method for Solid Fuel Combustion Zone During Sintering [E.F. Wegmann, T.V. Detkova, et al.; IZVESTIYA VYSSHIKH UCHEBNYKH ZAVEDENIY: CHERNAYA METALLURGIYA, No 1, Jan 92]	4
Optimization of Olenegorsk Concentrate Reduction Parameters in Devices With Swirling Fluidized Bed [D.I. Ryzhonkov, A.P. Kolgin, et al.; IZVESTIYA VYSSHIKH UCHEBNYKH ZAVEDENIY: CHERNAYA METALLURGIYA, No 1, Jan 92]	4
Amount and Composition of Gaseous Discharged During Pig Iron Tapping From Blast Furnace [A.V. Ganchev, O. Gonzales, et al.; IZVESTIYA VYSSHIKH UCHEBNYKH ZAVEDENIY: CHERNAYA METALLURGIYA, No 1, Jan 92]	4
Outlook for Metallurgical Dressing of Uenza and Bou-Hadr Deposit Iron Ores (Algeria) [Yu.S. Yusfin, Yu.B. Voytkovskiy, et al.; IZVESTIYA VYSSHIKH UCHEBNYKH ZAVEDENIY: CHERNAYA METALLURGIYA, No 1, Jan 92]	5
Efficiency of Desulfurizing Ladle Refining of Metal by Barium-Containing Reagents [V.P. Kirilenko, P.I. Yugov, et al.; IZVESTIYA VYSSHIKH UCHEBNYKH ZAVEDENIY: CHERNAYA METALLURGIYA, No 1, Jan 92]	5
Effect of Aluminum Content on Nonmetallic Inclusions in Nonstabilized Kh18N10 Stainless Steel [K. Michalek, M. Benda, et al.; IZVESTIYA VYSSHIKH UCHEBNYKH ZAVEDENIY: CHERNAYA METALLURGIYA, No 1, Jan 92]	5
Tribological Characteristics of Steel Surfaces With Laser Carbide Hardening Under Fluid Lubrication Friction Conditions [I.A. Vishnevetskaya, A.A. Ovchinnikov, et al.; IZVESTIYA VYSSHIKH UCHEBNYKH ZAVEDENIY: CHERNAYA METALLURGIYA, No 1, Jan 92]	6

Increasing Ductility Characteristics of Variable Cross Section Parts From KhN73MBTYu Alloy [S.B. Skachkov, L.N. Belyanchikov, et al.; IZVESTIYA VYSSHIKH UCHEBNYKH ZAVEDENIY: CHERNAYA METALLURGIYA, No 1, Jan 92]	6
Determining Limiting Gas Concentrations Under Metal Exposure to Vacuum and Inert Atmosphere [L.N. Belyanchikov, N.L. Belyanchikov; IZVESTIYA VYSSHIKH UCHEBNYKH ZAVEDENIY: CHERNAYA METALLURGIYA, No 1, Jan 92]	6
Decreasing Ingot Affectability With Scabs Under Bottom Casting of Steel [S.P. Yeronko, A.G. Savenko; IZVESTIYA VYSSHIKH UCHEBNYKH ZAVEDENIY: CHERNAYA METALLURGIYA, No 1, Jan 92]	7
Microstructure of Steel 06GMD at Subfreezing Temperatures [A.M. Skrebtsov, I.A. Dan, et al.; METALLOVEDENIYE I TERMICHESKAYA OBRABOTKA METALLOV, No 1, Jan 92]	7
Martensitic-Austenitic Steels for Making Tooling and Other Products in Instrument Engineering [V.G. Gorbach, I.V. Sidoruk, et al.; METALLOVEDENIYE I TERMICHESKAYA OBRABOTKA METALLOV, No 1, Jan 92]	7
Structure and Property Behavior of Steel 12Kh1MF Steam Superheater Metal During Operation Under Creep Conditions [N.V. Yelpanova, T.G. Berezina; METALLOVEDENIYE I TERMICHESKAYA OBRABOTKA METALLOV, No 1, Jan 92]	7

#### Nonferrous Metals, Alloys, Brazes, Solders

Scandium-Doped Aluminum Alloys [V.I. Yelagin, V.V. Zakharov, et al.; METALLOVEDENIYE I TERMICHESKAYA OBRABOTKA METALLOV, No 1, Jan 92]	9
Structure and Mechanical Properties of New VT25u High-Temperature Titanium Alloy [M.Ya. Brun, I.V. Soldatenko, et al.; METALLOVEDENIYE I TERMICHESKAYA OBRABOTKA METALLOV, No 1, Jan 92]	9
Effect of Hydrogen on Structure and Mechanical Properties of VT3-1 Titanium Alloy [B.A. Kolchayev, Yu.V. Poloskin, et al.; METALLOVEDENIYE I TERMICHESKAYA OBRABOTKA METALLOV, No 1, Jan 92]	9
Effect of Hydrogen on $\alpha$ - $\beta$ Transition Temperature in VT20 Alloy [Ye.V. Konopleva, V.M. Byazitov; METALLOVEDENIYE I TERMICHESKAYA OBRABOTKA METALLOV, No 1, Jan 92]	9

#### Nonmetallic Materials

Industrial Waste-Based Glass and Glass Ceramics [A.A. Ismatov, Kh.A. Abdullayev; STEKLO I KERAMIKA, No 1, Jan 92]	11
Ceramic Catalyst Carriers for Conducting Chemical Processes and Scrubbing Gas Discharges [Ye.Ya. Medvedovskiy, A.V. Fedotov, et al.; STEKLO I KERAMIKA, No 1, Jan 92]	11
High-Capacity Plate Glass Furnace Operation Analysis by Physical Modeling Method [I.M. Savina, V.P. Bespaiov, et al.; STEKLO I KERAMIKA, No 1, Jan 92]	11
Using Mathematical Model of Glass Density Prediction to Control Tank Furnace [R.I. Makarov, I.R. Dubov, et al.; STEKLO I KERAMIKA, No 1, Jan 92]	11
Effect of Shielding Atmosphere Composition on Adhesive Properties of Soda Lime Glass [V.F. Solinov, T.V. Kapiina, et al.; STEKLO I KERAMIKA, No 1, Jan 92]	12
Absorption Spectra of Staining Dopants in Glass From Synthetic Charge [A.B. Atkarskaya, V.I. Borulko, et al.; STEKLO I KERAMIKA, No 1, Jan 92]	12
Investigation of Low-Temperature Ceramics Firing Process by Electron Paramagnetic Resonance and Magnetostatic Methods [K.A. Kuvshinova, N.Yu. Yakubovskaya, et al.; STEKLO I KERAMIKA, No 1, Jan 92]	12
Ceramic Sheet Molding Method by Vacuum Filtration [M.K. Galperina, V.K. Kanayev, et al.; STEKLO I KERAMIKA, No 1, Jan 92]	13
Chain Structure Silicate-Based Ceramic Pigments [N.A. Sirazhiddinov, N.N. Akramova, et al.; STEKLO I KERAMIKA, No 1, Jan 92]	13
All-Ceramic Housing Parts of High-Temperature Electric Connectors [M.Yu. Khitrov, G.B. Sabun; STEKLO I KERAMIKA, No 1, Jan 92]	13

**Static and Cyclical Strength and Crack Resistance Characteristics of Welded Structural Steel Joints at Low Temperatures. Report 1**

927D0154A Kiev PROBLEMY POCHNOSTI  
in Russian No 2 (272), Feb 92 pp 17-22

[Article by V.V. Larionov, Kh.M. Khanukhov, N.I. Pidgurskiy, A.Ye. Voronetskiy, Central Scientific Research and Design Institute of Steel Structures, Moscow and Kemerovo; UDC 620.178.35]

[Abstract] Methods of engineering analysis of metalwork structures which operate at low ambient temperatures or cryogenic conditions and their behavior under static, impact, and cyclical loads are investigated. To this end, the effect of low (up to liquid nitrogen) temperatures on the static and low cycle strength and failure of steel 09G2S, 10KhSND, 06G2AF, 20KhGSA, 07Kh3GNMYuA and 0N6 is examined. The behavior of the ultimate strength with temperature, the behavior of ductility with temperature, the temperature dependence of the transverse deformation coefficient within the elastoplastic straining range, the low-temperature low cycle fatigue curves of steel and welded joints, and the behavior of the low cycle fatigue parameter under rigid loading and low temperatures are plotted. An expression for determining the low cycle fatigue index under rigid loading within a 293-113K range as a function of ductility with a decrease in temperature is derived on the basis of experimental data:  $m_e^T = m_e^{293K} - 0.047\Delta\psi^T$ . Figures 5; tables 2; references 8.

**Static and Cyclical Strength and Crack Resistance Characteristics of Welded Structural Steel Joints at Low Temperatures. Report 2**

927D0154B Kiev PROBLEMY POCHNOSTI  
in Russian No 2 (272), Feb 92 pp 22-27

[Article by V.V. Larionov, Kh.M. Khanukhov, N.I. Pidgurskiy, A.Ye. Voronetskiy, Central Scientific Research and Design Institute of Steel Structures, Moscow and Kemerovo; UDC 620.178.35]

[Abstract] It is shown that low cycle fatigue strength and failure data on structural steels at low temperatures may be used for analyzing cyclically loaded metalwork structures on the basis of deformation criteria at the crack formation stage. The cracking characteristics of structural steels and their welded joints under static, cyclical, and impact loading are examined within a broad temperature range; in so doing, attention is focused on crack resistance of welded joints since it is the principal factor which limits the normal life of metalwork structures; the welded joints localize the main defects and thus predetermine the development of fatigue cracks under repeat loading. The critical values of the notch sensitivity index under cyclical and dynamic loading of the principal zones of welded joints from steel 20K, 09G2S, 0N6, 12KhGDAF, 10KhSND, 06G2AF, 20KhGSA, and 07Kh3GNMYuA are determined within a 293-113K temperature range. The correlation between the crack

resistance  $C$  and  $n$  parameters and the dependence of the fatigue crack propagation rate on the sample temperature are plotted. Welded joints are studied by making a notch in the base metal (OM), weld metal (MSh), and the heat affected area (ZTV). The crack resistance data thus found may be used as the characteristics of materials for various approaches to assessing the service life and formulating the low-temperature criteria of metal structures under cyclical loading. Figures 4; tables 2; references 15: 14 Russian, 1 Western.

**Long-Term Strength of Welded Pipeline T-Joints**

927D0154C Kiev PROBLEMY POCHNOSTI  
in Russian No 2 (272), Feb 92 pp 40-45

[Article by R.Z. Shron, E.I. Getsfrid, S.Yu. Googe, I.F. Nebesova, L.V. Voronkova, Urals Department of the All-Union Scientific Research Institute of Heat Engineering; UDC 621.181.021:621.791.05: [539.434+539.376]]

[Abstract] Since the reliability and service life of pipeline systems are largely limited by the damage to welded T-joints (TSS), large-scale models of pipeline T-joints under internal pressure at a temperature of 600°C are examined experimentally in test benches. To this end, pipes from 12Kh1MF heat resistant steel are welded by the E-09Kh1MF and E-09Lh1M electrodes according to GOST 9467-75. The joints and welds are examined metallographically. The finite element method (MKE) and an elastic creep approximation method (Neubur method) are used to analyze the stressed state of the tee. The dependence of the notch sensitivity index on the union and tube branch diameter ratio and the dependence of the notch sensitivity index on the union and tube wall thickness are plotted. A procedure for estimating the taut strained state of pipeline T-joints under internal pressure and creep conditions is formulated. The strength estimate produced by the procedure and the results of test bench experiments confirm that the load carrying capacity of such joints may be lower by almost twofold than that of tubes of the same size not weakened by a hole and welded joint. Figures 7; references 8.

**Method of Measuring Equivalent Stresses in Aircraft Gas Turbine Engine Blades**

927D0154D Kiev PROBLEMY POCHNOSTI  
in Russian No 2 (272), Feb 92 pp 45-48

[Article by V.V. Malygin (deceased), D.F. Fedorchenko, S.R. Zalautdinov, Trud Scientific Production Association; UDC 621.45.037.253.5:539.4]

[Abstract] The need for statistical evaluation of the damage potential of stochastic vibratory processes to aircraft gas turbine engine (GTD) blades and the inadequacy of existing methods of reducing stochastic processes to equivalent harmonic processes are discussed and a new method of analytical and experimental measurement of equivalent stress is proposed; the method

enables us to use relatively simple methods to attain the desired results without substantially increasing the duration of analyzing the data of test bench dynamic strain measurement. The real and simulated vibratory stress process and real and simulated vibration stresses in the blades and vanes are plotted. It is assumed that during the steady-state vibratory process realization time, the harmonic spectrum of the stochastic vibrations remains constant and that there exists a time period during which the stochastic vibration amplitude changes insignificantly, i.e., all vibration cycles have a constant amplitude. Pilot operation of the analytical experimental method demonstrates that its implementation does not significantly increase the outlays of CPU time for analyzing strain processes and increases the reliability and soundness of the safety margin estimates. Figures 3; references 5; 4 Russian, 1 Western.

#### **Effect of Heat Treatment on Hydrogen Embrittlement Resistance of Age Hardenable Nickel Alloy**

927D0161D Moscow METALLOVEDENIYE I  
TERMICHESKAYA OBRABOTKA METALLOV  
in Russian No 1, Jan 92 pp 17-20

[Article by K.A. Yushchenko, V.S. Savchenko, O.N. Ostapenko, Electric Welding Institute imeni Ye.O. Paton; UDC 669.14.018.44:539.56]

[Abstract] Extensive uses of hydrogen as fuel prompted studies of its effect on the structure and properties of various structural materials; the mechanical properties and toughness parameters of the 03Kh20N60MVYu (EP901) age hardenable alloy used in structures operating within a -269 to +750°C temperature range in hydrogen-containing media are investigated after various heat treatment conditions. The chemical composition of the actual alloy, its composition specifications, and heat treatment conditions are summarized. The delayed fracture curves of the 03Kh20N60MVYu after various heat treatment conditions and mechanical properties of the 03Kh20N60MVYu alloy after various heat treatment conditions are plotted and a typical macrofracture of the 03Kh20N60MVYu alloy is examined under a microscope after heat treatment. An analysis shows that extended exposure to a hydrogen-containing medium and loading affect the character of alloy failure

and the crack propagation in the samples. Alloy failure in a hydrogen medium is intercrystalline and the cracks form along the grain boundary during the entire testing process. Austenization at a 1,050°C temperature for one hour, cooling in the air, plus aging at 750°C for three hours facilitate the development of a structure with uniformly distributed  $\gamma'$ -phase particles whose dimensions differ little from the mean and is thus an optimum heat treatment condition for decreasing the hydrogen embrittlement since hydrogen diffusivity decreases significantly after the  $\gamma'$ -phase precipitation at 700°C. Figures 4; tables 2; references 9.

#### **Structure and Properties of Titanium Alloys With Nitrogen**

927D0161M Moscow METALLOVEDENIYE I  
TERMICHESKAYA OBRABOTKA METALLOV  
in Russian No 1, Jan 92 pp 45-46

[Article by B.Ye. Paton, B.I. Medovar, G.M. Grigorenko, K.G. Grigorenko, Electric Welding Institute imeni Ye.O. Paton and Kiev Polytechnic Institute; UDC 669.295.5'786]

[Abstract] Published data on the structure and properties of titanium nitrides are classified and the results of an investigation of the structure and microhardness of massive cast nitrides produced by an original method of titanium smelting by an electric arc in an atmosphere of nitrogen are cited. A constitution diagram of the Ti-N system is shown and discussed and the four main methods of producing titanium nitride are summarized. The structural components of the surface hardened layer are identified under an ISM-840 electron microscope made by JEOL (Japan) with a wave microprobe for detecting light elements at a 30 kV accelerating potential. The alloy microhardness is measured by an R-400 microhardness gauge made by LECO (USA). The results show that microhardness increases at the grain boundaries. The high melting point and hardness and specific features of the structural and phase composition as well as the possibility of producing cast titanium nitride in castings, ingots, and surfaced layers of various shape and size make this composite material suitable for subsequent machining and treatment. Figures 2; references 9; 7 Russian, 2 Western.



### Recrystallization of Multilayer CoNi/Cr Films

927D0161N Moscow METALLOVEDENIYE I  
TERMICHESKAYA OBRABOTKA METALLOV  
in Russian No 1, Jan 92 pp 46-48

[Article by G.N. Kadykova, T.K. Lyakhovich, I.I. Khvostikova, Moscow Institute of Electronic Engineering and Vacuum Tube and Instrument Scientific Production Association; UDC 539.216.2:621.318]

[Abstract] The possibility of improving the magnetic properties of hard discs (ZhMD) by heat treatment and increasing the recording density (TPI) by increasing the coercive force of the working layer are discussed and the effect of the annealing conditions on the structure and properties of  $\text{Co}_{80}\text{Ni}_{20}/\text{Cr}$  films applied to a glass substrate by the method of electron beam sputtering is investigated; the Cr sublayer is 500 nm thick and the CoNi sublayer is 50 nm thick. The magnetic properties of the film are measured in a vibratory magnetometer,

X-ray analyses are performed by a DRON-2 diffractometer in  $\text{CuK}$  radiation, and the film surface relief is examined under a REM-100U electron microscope. The films are annealed in a  $10^{-1}$  Pa vacuum at a 250-350°C temperature for three hours. The nonannealed films have a predominant Cr(100) orientation while the structure and properties of the CoNi layer are different. X-ray diffraction patterns of the films in the initial state and after annealing are plotted and the coercive force and hysteretic properties are summarized. An analysis of the findings indicates that CoNi/Cr films heated to a 250-350°C temperature recrystallize forming a new structure whereby the Co(1011)/Cr(110) orientation changes to Co(1120)/Cr(100) while the grain size remains virtually unchanged. The grains begin to grow only with subsequent heating. The change in the CoNi/Cr film orientation as a result of its recrystallization leads to an increase in the coercive force to 60 kA/m and the  $B_r/B_m$  ratio to 0.96, primarily due to a transition of the axis of easy magnetization of [0001]CoNi to the film plane. Figures 2; tables 1; references 5: 1 Russian, 4 Western.

### Relative Error of Measuring Oxygen Activity in Liquid Steel by Electrochemical Transducers

927D0152A Moscow IZVESTIYA VYSSHIKH UCHEBNIKH ZAVEDENIY: CHERNAYA METALLURGIYA in Russian No 1, Jan 92 pp 1-4

[Article by I.V. Zinkovskiy, Yu.I. Nebosov, V.M. Skosyrev, Central Scientific Research Institute of Ferrous Metallurgy and Moscow Steel and Alloy Institute; UDC 621.3.088]

[Abstract] The methods of measuring the oxygen activity in liquid steel by UKOS-type transducers which convert the electromotive force developing on the sensor immersed in the melt into the value of oxygen activity and the factors affecting the measurement error of this method are discussed and two problems involved in estimating the relative measurement error are formulated: To estimate the proximity of a series of paired measurements and using the random emf error of a series of paired measurement, determine the confidence interval of a single measurement. The results of paired measurements by DOSP oxidation transducers are summarized and the maximum measured oxygen activity errors of DOSP transducers at a 1,600°C temperature are calculated. On this basis, the standard deviations  $S_{\Delta}$  of the O activity measured in deoxidized and nondeoxidized metal by one, two, and ten DOSP transducers are computed: 3.95 percent for nondeoxidized steel and 0.79 percent for carbon-deoxidized carbonyl iron. The use of UKOS units with DOSP transducers makes it possible to decrease the measurement error by almost threefold; an increase in the number of measurements does not further increase the measurement accuracy. Tables 2; references 2: 1 Russian, 1 Western.

### Improved Heat Balance Analysis Method for Solid Fuel Combustion Zone During Sintering

927D0152C Moscow IZVESTIYA VYSSHIKH UCHEBNIKH ZAVEDENIY: CHERNAYA METALLURGIYA in Russian No 1, Jan 92 pp 8-12

[Article by E.F. Wegmann, T.V. Detkova, Dube Ndabezinkhle, Moscow Steel and Alloy Institute; UDC 669.162.12:622.785]

[Abstract] A known procedure of analyzing the heat balance in the solid fuel combustion zone during the agglomeration sintering and the importance of this procedure in the case of two-layer or two-zone combustion for estimating the development of fuel and charge ore component segregation and optimizing the sintered layer height and the intensity of its additional heating are discussed and an improved analysis method is proposed. The old procedure is complemented by taking into account the degree of the burning carbon fuel graphitization, the effect of hygroscopic moisture under the combustion zone, the mass-averaged temperature of sintering mixture lumps and particles, the silicate charge residue crystallization heat, and the nonuniformity of the combustion zone. The temperature distribution in

the combustion zone, change in the vertical sintering rate during the sintering process, and minimum possible specific rates of solid fuel during sintering are plotted and the quantity of regenerated heat per 100 kg of sinter is summarized. The improved method makes it possible to calculate the total heat transfer coefficient during the heat exchange between the ready sinter cake and the air above the combustion zone and determine the temperature of any sinter cake layer after sintering and the temperature of the ready sinter cake as a whole. Figures 3; tables 1; references 6: 4 Russian, 2 Western.

### Optimization of Olenegorsk Concentrate Reduction Parameters in Devices With Swirling Fluidized Bed

927D0152D Moscow IZVESTIYA VYSSHIKH UCHEBNIKH ZAVEDENIY: CHERNAYA METALLURGIYA in Russian No 1, Jan 92 pp 12-13

[Article by D.I. Ryzhonkov, A.P. Kolgin, S.B. Kostyrev, A.V. Vasilyev, A.B. Savin, Moscow Steel and Alloy Institute; UDC 669.181.4]

[Abstract] The effect of various factors on the critical space ratio of devices with a swirling fluidized bed created by a rotary magnetic field—the most important parameter characterizing the efficiency of the ore concentrate reduction in a reactor—is investigated; to this end, the effect of partial magnetite magnetization and its fraction by mass on the critical space ratio is examined at the Olenegorsk Ore Dressing Combine using a concentrate with 72 percent Fe and less than 1 percent of impurities with a fraction of larger than 0.064 mm. The ore concentrate is reduced in a device with fluidized swirling bed with hydrogen at a 500°C temperature until attaining a specified degree of metallization. The dependence of the critical space factor, i.e. the ratio of the maximum amount of ferromagnetic material forming a stable swirling bed to the reactor volume, on the degree of preliminary concentrate metallization at various fractions of magnetite concentration in the mixture and the dependence of the maximum particle strand length on the reduction degree at specified strand length to particle diameter ratios are plotted. The critical ratio increases with an increase in the metallization degree due to an increase in the material's magnetization and an improvement in the charge stirring conditions. Figures 2; references 5.

### Amount and Composition of Gaseous Discharged During Pig Iron Tapping From Blast Furnace

927D0152E Moscow IZVESTIYA VYSSHIKH UCHEBNIKH ZAVEDENIY: CHERNAYA METALLURGIYA in Russian No 1, Jan 92 pp 13-14

[Article by A.V. Ganchev, O. Gonzales, V.M. Chizikova, I.F. Kurunov, I.A. Nikitina, Moscow Steel and Alloy Institute; UDC 669.1:628.5]

[Abstract] The shortcomings of experimental methods of measuring the volume and composition of the gases discharged during the tapping of pig iron from blast furnaces due to the low concentration of certain components are outlined and a new method of determining the amount and composition of gaseous discharges which makes it possible to obtain sufficiently full data on the thermodynamically feasible gaseous phase composition for specified cast iron contents and temperatures is presented. The two-phase air-pig iron system is investigated within a 1,300-1,600°C temperature range by the method of mathematical modeling using the ASTRA multiobjective software package which is based on the principle of calculating the equilibria in closed heterogeneous systems from the entropy maximum. The release of various gases per ton of pig iron during tapping at various temperatures is summarized and the discharge of harmful sulfurous compounds as a function of the sulfur content in pig iron is plotted. Thus, a thermodynamic analysis of the pig iron tapping process makes it possible to identify a wide range of chemical compounds harmful to human health. The dependence of the level of toxic discharges on the pig iron content makes it possible to outline measures for improving working conditions in the foundry. Figures 1; tables 1; references 3.

#### **Outlook for Metallurgical Dressing of Uenza and Bou-Hadr Deposit Iron Ores (Algeria)**

927D0152F Moscow IZVESTIYA VYSSHIKH  
UCHEBNIKH ZAVEDENIY: CHERNAYA  
METALLURGIYA in Russian No 1, Jan 92 pp 15-16

[Article by Yu.S. Yusfin, Yu.B. Voytkovskiy, Z. Labed, T.N. Bazilevich, M.L. Kharakhan, Moscow Steel and Alloy Institute; UDC 622.781]

[Abstract] The characteristics of iron ores from the Uenza and Bou-Hadr deposits in Algeria, particularly the presence of more than 2 percent Mn which limits the range of possible brands of steel and lowers the competitiveness of the metallurgical works, are discussed and it is noted that attempts to refine the raw wet ore are unsuccessful due to its low magnetic characteristics. It is reported that magnetizing roasting makes it possible substantially to improve the ore's magnetic characteristics, and particularly increase its magnetic susceptibility by 320 times. The results of three versions of ore roasting and five versions of magnetic dressing are summarized in order to establish the optimum process conditions and the gamma-resonance spectrum of the original Uenza ore is plotted. It is shown that the magnetic fraction yield increases sharply with the roasting temperature and magnetic field strength. It is suggested that further experiments be aimed at examining the reduction characteristics of naturally Mn-alloyed iron oxides and the elemental composition of the gangue. Figures 1; tables 1.

#### **Efficiency of Desulfurizing Ladle Refining of Metal by Barium-Containing Reagents**

927D0152G Moscow IZVESTIYA VYSSHIKH  
UCHEBNIKH ZAVEDENIY: CHERNAYA  
METALLURGIYA in Russian No 1, Jan 92 pp 22-25

[Article by V.P. Kirilenko, P.I. Yugov, V.M. Zhuravlev, V.I. Savchenko, Central Scientific Research Institute of Ferrous Metallurgy; UDC 669.18.046.5]

[Abstract] The need for deep desulfurizing of metal in the ladle in order to produce cold-resistant steel for gas pipelines prompted a study of the efficiency of desulfurizing ladle refining by barium-containing powder reagents. To this end, the parameters of desulfurizing refining of low alloyed steel 09G2FB containing no more than 0.006 percent S are examined and the use of silicobarium in place of silicocalcium for this purpose is discussed. The sulfide capacity behavior of synthetic slag during the refining, the ratio of the oxygen and sulfur activity in liquid iron as a function of temperature for a sulfide-oxide equilibrium, the oxygen activity behavior during the metal refining, and the sulfur distribution coefficient behavior during the ladle refining are plotted. An analysis of the findings demonstrates that by comprehensive metal ladle refining with Ba-containing reagents together with manipulating the metal oxidation in the converter and regulating the iron deoxidation with aluminum, as well as maintaining the necessary temperature of the metal and compensating for the harmful effect of the lining erosion make it possible effectively to remove sulfur from the liquid metal and decrease the sulfur concentration in ready steel. Figures 4; references 5.

#### **Effect of Aluminum Content on Nonmetallic Inclusions in Nonstabilized Kh18N10 Stainless Steel**

927D0152H Moscow IZVESTIYA VYSSHIKH  
UCHEBNIKH ZAVEDENIY: CHERNAYA  
METALLURGIYA in Russian No 1, Jan 92 pp 29-31

[Article by K. Michalek, M. Benda, R. Raclavski, Ostrava Mining Institute, Czechoslovak Republic; UDC 669.046.558:669.71]

[Abstract] The effect of the origin of nonmetallic inclusions on the behavior of nonstabilized Kh18N10 stainless steel is discussed and the effect of the aluminum content on the composition of oxide and sulfide inclusions in this steel is investigated; in so doing, attention is focused on the total degree of steel contamination with nonmetallic inclusions. For this purpose, pilot smeltings are made in a 36-kg open induction furnace with a MgO- and Al<sub>2</sub>O<sub>3</sub>-based lining. The residual aluminum and total oxygen concentration in ten samples taken from the ladle are summarized and the effect of the residual aluminum concentration on the Cr and Al content in oxide inclusions and the ratio of the residual Al content and total inclusion area in the samples are plotted and the quantity of inclusions in samples as a function of



particle size is compared. The morphology and chemical content of the nonmetallic inclusions are examined under a Neophot-2 microscope and JEOL 35CF-LINK 860 X-ray microanalyzer. The study shows that the morphology, chemical composition, and total area of inclusions in samples of nonstabilized stainless steel Kh18N10 containing approximately 0.25 percent Mn largely depend on the Al content; the contamination degree can be minimized, the undesirable chromium, manganese, and iron oxide-based impurities can be limited, and the  $Al_2O_3$  clusters can be eliminated by maintaining the Al concentration within a 0.018-0.037 percent range. Figures 3; tables 1; references: 6 Western.

### **Tribological Characteristics of Steel Surfaces With Laser Carbide Hardening Under Fluid Lubrication Friction Conditions**

927D0152I Moscow IZVESTIYA VYSSHIKH UCHEBNIKH ZAVEDENIY: CHERNAYA METALLURGIYA in Russian No 1, Jan 92 pp 86-88

[Article by I.A. Vishnevetskaya, A.A. Ovchinnikov, V.N. Gladkova, Khmel'nikskiy Technological Institute; UDC 620.172:621.9.048]

[Abstract] The task of examining the tribological characteristics of laser-hardened surfaces after their finishing treatment by grinding is formulated and it is noted that each individual study should be comparative, i.e., the characteristics of poorly known new materials or coats must be compared to similar characteristics of layers produced by traditional and popular technologies measured under the same conditions. The tribological characteristics of laser-hardened samples of structural steels 40Kh, 38KhA, and U8, corrosion-resistant martensitic steel 95Kh18, and high-temperature steel EI-69 (4Kh14N14V2M) are examined; for comparison, case-hardened and nitrided samples of steel 12KhN3A and 38KhMYuA as well as EI-69 are tested. The characteristic microstructure of the surface layers modified by a TiC/Ni and VK-25 powder is examined under a microscope, the dependence of the linear wear rate on the specific load during normal wear periods of steel 38KhA samples hardened by a TiC/Ni powder is plotted, and the load, wear rate, and friction coefficient of various hardened materials on different bases after different types of machining are summarized. An analysis of the findings demonstrates that the high quality of surface after polishing, the absence of porosity, and an increase in wear resistance indicate that the methods of laser hardening and carbide particle injection into the surface are quite competitive albeit extended and labor-consuming chemical-heat treatment processes for conditioning local areas of surface parts operating under the conditions of fluid lubrication friction. The development of layers with laser carbide hardening on structural steels decreases the wear rate by 1.5-2.5 times compared to gaseous case hardening and nitriding. Figures 2; tables 1; references 2: 1 Russian, 1 Western.

### **Increasing Ductility Characteristics of Variable Cross Section Parts From KhN73MBTYu Alloy**

927D0152J Moscow IZVESTIYA VYSSHIKH UCHEBNIKH ZAVEDENIY: CHERNAYA METALLURGIYA in Russian No 1, Jan 92 pp 113-115

[Article by S.B. Skachkov, L.N. Belyanchikov, G.I. Doronin, Moscow Steel and Alloy Institute; UDC 669.187.26]

[Abstract] The low ductility of nickel-based alloys which limits their uses prompted the development of the VADER process which makes it possible to increase ductility by forming a fine-grain equiaxial macrostructure; yet only cylindrical ingots can be produced by the VADER process. Thus, experiments aimed at increasing the ductility of the KhN73MBTYu nickel-containing alloy, particularly parts with a variable cross section, are carried out at the Moscow Steel and Alloy Institute (MISI). The remelting conditions in an atmosphere of helium and the resulting macrostructure are described; the results show that a fine-grain equiaxial dendritic structure with a 0.0002-0.0003 m grain is formed. The experiments made it possible to make a casting from the KhN73MBTYu alloy with a variable cross section and a uniform fine-grain structure throughout the volume; the ductility characteristics of the casting exceed those of parts made by the conventional vacuum arc remelting method by 25-28 percent. Figures 1; tables 1; references 1.

### **Determining Limiting Gas Concentrations Under Metal Exposure to Vacuum and Inert Atmosphere**

927D0152K Moscow IZVESTIYA VYSSHIKH UCHEBNIKH ZAVEDENIY: CHERNAYA METALLURGIYA in Russian No 1, Jan 92 pp 115-116

[Article by L.N. Belyanchikov, N.L. Belyanchikov, Moscow Steel and Alloy Institute; UDC 669.187.4]

[Abstract] The limiting gas concentration—the value which the dissolved gas concentration approaches when the metal is exposed to a vacuum—is defined and formulas are derived for the limit of nitrogen and hydrogen concentration assuming that in a vacuum the process is bounded by the internal mass transfer (VM) and chemical desorption link (KhDZ). It is shown that the use of an inert atmosphere which suppresses the vaporization processes improves the conditions for attaining ultralow gas concentration in the metal; formulas are derived for calculating the nitrogen and hydrogen concentration in a deep dynamic or chemical vacuum, making it possible to estimate the limit of gas concentrations under metal exposure to a vacuum or an inert atmosphere on the basis of thermodynamic and kinetic factors. References 2.

### Decreasing Ingot Affectability With Scabs Under Bottom Casting of Steel

927D0152L Moscow IZVESTIYA VYSSHIKH UCHEBNIKH ZAVEDENIY: CHERNAYA METALLURGIYA in Russian No 1, Jan 92 pp 116-117

[Article by S.P. Yeronko, A.G. Sayenko, Donetsk Polytechnic Institute; UDC 621.765.5]

[Abstract] The effect of the steel gushing on the development of scabs in bottom cast ingots and methods of eliminating the metal surface vibration are discussed and it is suggested that a metal repeller mounted over the ingot mold plate be used to quench the melt jet. The shape and principal geometric parameters of the repeller are determined by investigating a model of an eight ton ingot mold (on a 1:5 scale); to this end, the hydrodynamic processes occurring during the filling of the ingot mold bottom with a liquid are examined for various repeller designs. Statistical processing of the results of pilot and comparative smeltings attests that rejections due to ingot scabs can be reduced by 1.2 times by adding the repeller. Figures 1; references 3.

### Microstructure of Steel 06GMD at Subfreezing Temperatures

927D0161A Moscow METALLOVEDENIYE I TERMICHESKAYA OBRABOTKA METALLOV in Russian No 1, Jan 92 pp 6-7

[Article by A.M. Skrebtsov, L.A. Dan, G.S. Lupandin, Mariupol Metallurgical Institute and Mariupol Branch of the Prometheus Scientific Research Institute of Composites; UDC 669.14.001.5]

[Abstract] The behavior and microstructure of low pearlitic steel 06GMD intended for making units and parts of machines operating in the far north are examined; the microstructure is studied at various temperatures in the cast and hot-rolled state and in the hot-rolled state 24 hours after the treatment. The samples for the study are cut from cast club-shaped specimens made from hot-rolled sections with subsequent normalizing. The microstructure at normal and subfreezing temperatures is examined in an ALA-TOO (IMASH-20-75) unit after pickling the samples in a 3 percent  $\text{HNO}_3$  solution and under an MVT-1 microscope. The study reveals that the ferrite grains in the cast samples of hot-rolled steel 06GMD are reversibly refined at temperatures below  $0^\circ\text{C}$ ; it is speculated that this phenomenon is due to the thermal compression of the metal with a decrease in temperature. Figures 1.

### Martensitic-Austenitic Steels for Making Tooling and Other Products in Instrument Engineering

927D0161B Moscow METALLOVEDENIYE I TERMICHESKAYA OBRABOTKA METALLOV in Russian No 1, Jan 92 pp 7-9

[Article by V.G. Gorbach, I.V. Sidoruk, I.N. Melkumov, S.B. Birin, Kiev Polytechnic Institute, Electric Furnace

Steel Metal Works, and Tekhnopribor Scientific Production Association, Riga; UDC 669.14.018.6]

[Abstract] The martensitic-austenitic steels which, in contrast to maraging steels, do not contain cobalt are divided into two categories: those which contain 24-27 percent Ni and have a metastable austenite structure after hardening and those which contain 16-21 percent Ni and have a packed martensite structure after hardening. The properties of pilot and commercial martensitic-austenitic steels of the latter category are investigated; these steels are cheaper and have the same level of mechanical properties yet are somewhat inferior to the first group with respect to deformability in the nonhardened state. The chemical composition of the steel samples under study is summarized. The dependence of the ultimate rupture strength, ductility, elasticity modulus, and coercive force of steel N26YuT2B on the aging temperature (1 h long), the effect of the aging temperature (1 h long) on the mechanical properties of steel N21M2T2B after water quenching at a  $900^\circ\text{C}$  temperature, and the effect of the aging temperature (1 h long) on the service life of steel N21M2T2B under symmetric tension and compression at a  $\pm 450 \text{ N/mm}^2$  load at a 750 cycles/min frequency are plotted. The study shows that type N19M2T2B steels have a 530-560 HV hardness, a 1,760-1,900  $\text{N/mm}^2$  rupture strength, an 8-10 percent elongation, and a 40-50 percent ductility, as well as a high fatigue strength, thermal cycling strength, and corrosion resistance. The optimum range of mechanical, elastic, and magnetic properties of these steels is attained due to age hardening within the  $\alpha\text{--}\gamma$  transformation range; these steels may be used for making die casting molds for nonferrous metals and polymers. Figures 3; tables 2; references 7.

### Structure and Property Behavior of Steel 12Kh1MF Steam Superheater Metal During Operation Under Creep Conditions

927D0161E Moscow METALLOVEDENIYE I TERMICHESKAYA OBRABOTKA METALLOV in Russian No 1, Jan 92 pp 21-23

[Article by N.V. Yelpanova, T.G. Berezina, Chelyabengergo Production Association and All-Union Advanced Training Institute for the Energy Ministry Technical Staff; UDC 669.14.018.44:620.172.251.2]

[Abstract] The behavior patterns of the structure, phase composition, and service properties of steel 12Kh1MF during 50-200,000 hours of operation under a 10-24 MPa steam pressure at a  $550\text{--}600^\circ\text{C}$  temperature are discussed and the kinetics of structure, carbide phase composition, and high-temperature strength of steel 12Kh1MF superheaters during extended operation under creep conditions are investigated. The alloying element redistribution between the solid solution and carbide phases is examined and the behavior of the Cr and Mo concentration in the solid solution as a function of the Larson-Mueller parameter  $P = T(\lg t + 20)$ , the dependence of the most likely carbide particle size as a

function of the temperature-time parameter  $P$ . The dependence of the structural components' microhardness and microhardness differential on the parameter  $P$ , and the long-term strength curves of the superheater pipe metal for failed pipes and on the basis of test data are plotted. The conclusion is drawn that extended

operation under creep conditions leads to a loss of strength and a decrease in the high-temperature strength of steel, it is recommended that the long-term strength curve plotted on the basis of operational fractures be used for increasing the accuracy of superheater pipe life forecasting. Figures 4; references 4.

### Scandium-Doped Aluminum Alloys

927D01614 Moscow METALLOVEDENIYE I  
TERMICHESKAYA OBRABOTKA METALLOV  
in Russian No. 1, Jan 92 pp 74-78

[Article by V.I. Yelagin, V.V. Zakharov, L.I. Rudakov.  
UDC 669.745.743]

[Abstract] The effect of doping with scandium—a strong inoculant of the cast grain structure at certain levels—on the structure and properties of aluminum alloys is discussed and the principal metallurgical principles of Sc-doping of aluminum alloys are investigated. In this and the findings of many years of research in these fields and published data are summarized. The issues of selecting the optimum scandium concentration range in aluminum alloys, additionally doping Sc-doped aluminum alloys with zirconium and such transition metals as manganese, titanium, chromium, vanadium, and hafnium, and the relationship between Sc and the principal alloying constituents used in commercial aluminum alloys are addressed. An analysis of the intermetallic solid solution decay and the behavior of mechanical properties of aluminum alloys with various additions makes it possible to recommend that Sc be added to aluminum alloy in the amount of 0.1-0.3 percent together with 0.05-0.15 percent of which enhances scandium's positive effect on the structure and mechanical properties. The best results are attained in Sc-doped alloys which do not contain constituent capable of binding scandium into insoluble phases, e.g., Mg, Zn-Mg, and Mg-Li; if the copper composition is limited to 1.5 percent, it is possible to add Sc and Zr to Al-Zn-Mg-Cu and Al-Cu-Li alloys. Figures 8; tables 2; references 16; 15 Russian, 1 Western.

### Structure and Mechanical Properties of New VT25u High-Temperature Titanium Alloy

927D01616 Moscow METALLOVEDENIYE I  
TERMICHESKAYA OBRABOTKA METALLOV  
in Russian No. 1, Jan 92 pp 29-31

[Article by M.Ya. Brun, I.V. Soldatenko, L.A. Bykova.  
UDC 669.295.5:620.17:620.181]

[Abstract] The structure and mechanical properties of the new VT25u  $\alpha + \beta$  titanium superalloy developed at the All-Union Institute of Aviation Materials (VIAM) which has higher long-term and ultimate strength at a 500-550°C temperature than commercial alloys and is intended for making aviation engine disks and blades are investigated. To this end, rolled rods with an 18 mm diameter and a globular structure are examined. The effect of the  $\beta$ -grain size on the mechanical properties of the VT25u alloy, the effect of the cooling rate on the mechanical properties of the VT25u alloy, and the dependence of the mechanical properties of the bars with a globular structure on the ultimate strength level are plotted; the silicide particles in bars and fractures are examined under a microscope and radiographically. The findings indicate that the VT25u structure is typical of  $\alpha + \beta$

$\alpha + \beta$  alloys and is characterized by a higher constituent grain size due to the presence of tungsten which greatly lowers silicide formation rate. The effect of the VT25u structure on the mechanical properties is also similar to the effect of  $\alpha + \beta$  titanium commercial alloys. VT25u is characterized by a higher structural sensitivity of ductility and toughness, 600000, due to the silicide particles which have a diameter of 0.1-0.2  $\mu$ m. They are located predominantly in the grain boundaries. The optimum combination of mechanical properties is obtained for the ultimate strength at room temperature of  $10^5$  MPa between 1,120 and 1,200°C, 10-15 percent, G.V. Korzhova, V.V. Leonov, L.S. Pletinskaya, and Ye.M. Golubeva participated in the study. Figures 4; tables 1; references 6.

### Effect of Hydrogen on Structure and Mechanical Properties of VT3-1 Titanium Alloy

927D01617 Moscow METALLOVEDENIYE I  
TERMICHESKAYA OBRABOTKA METALLOV  
in Russian No. 1, Jan 92 pp 32-34

[Article by A.A. Yelagin, L.S. Pletinskaya, V.I. Sedov, Ye.B. Yegorov, A.G. Rudakov. Scientific Research Institute of Aviation Materials and Stupino Department of the Moscow Aviation Engineering Institute.  
UDC 669.295.5:620.17:620.181]

[Abstract] The effect of hydrogen permeation on the structure and mechanical properties of the VT3-1 titanium alloy  $\alpha + \beta$  rods of 10 mm dia. rods of the VT3-1 alloys are subjected to tensile tests at a  $3.3 \cdot 10^{-3}$  s<sup>-1</sup> rate and toughness tests at a  $10^{-2}$  s<sup>-1</sup> straining rate. The samples for the study are hydrogen treated in a gaseous hydrogen medium at an 800°C temperature to a 10<sup>-2</sup> s<sup>-1</sup> straining rate. The dependence of the ultimate strength and dynamic strength on the hydrogen concentration, the dependence of elongation on the hydrogen concentration at various temperatures, and the temperature behavior of toughness in alloys with various hydrogen concentrations are plotted. Test data demonstrate that titanium alloy doping with hydrogen in the amount of 0.001 percent may facilitate the cutting conditions, improve deformability, and reduce toughness at the turning temperature (700-950°C). In addition, as a result of hydrogen absorption, alloy chips become more brittle after cooling and are thus easier to crush for subsequent processing. Figures 4; references 2.

### Effect of Hydrogen on $\alpha \rightarrow \beta$ Transition Temperature in VT20 Alloy

927D01618 Moscow METALLOVEDENIYE I  
TERMICHESKAYA OBRABOTKA METALLOV  
in Russian No. 1, Jan 92 pp 35-37

[Article by Ye.V. Konopleva, V.M. Bvazitov, General and Zhiganskoy Chemistry Institute at the USSR Academy of Sciences. UDC 669.295.5:620.17:620.181.4]

[Abstract] The phenomenon of titanium alloy plasticization as a result of hydrogen absorption—an opposite of

hydrogen embrittlement—is discussed and the effect of hydrogen on the temperature of the  $\alpha$ — $\beta$  transition in the VT alloy with various hydrogen concentrations under continuous heating conditions is investigated. The alloy composition is summarized. The VT20 alloy is hydrogen-treated at an 800°C temperature using a procedure described in *Fizika metallov i metallovedeniye* Vol. 76 No. 5, 1989, p. 993. As a result, three alloys are produced containing 0.16, 0.45, and 0.83 percent H. The temperature ranges of phase transitions are determined with the help of a Lineis dilatometer and by differential thermal analysis (DTA). The differential thermal analysis curves of the VT20 alloy without hydrogen and with

0.16 and 0.45 percent H and the dependence of the  $\alpha$ — $\beta$  transition temperature under continuous heating on the hydrogen concentration are plotted. The microstructure of the alloy is examined under a microscope. The results show that addition of 0.16, 0.45, and 0.83 percent H lowers the  $\alpha$ — $\beta$  transition temperature in proportion to the hydrogen concentration; yet the phase transition in hydrated VT20 alloy under continuous heating occurs at much higher temperatures than those at which hydrogen plasticization was observed by Ye.G. Ponyatovskiy and I.O. Bashkin. The authors are grateful to Ye.G. Ponyatovskiy and I.O. Bashkin for discussing the findings and making suggestions. Figures 3; references 5



### Industrial Waste-Based Glass and Glass Ceramics

927D0153A Moscow STEKLO I KERAMIKA  
in Russian No 1, Jan 92 pp 2-3

[Article by A.A. Ismatov, Kh.A. Abdullayev, Tashkent Polytechnic Institute; UDC 666.11:666.263.2:666.004.8]

[Abstract] The easy availability and low cost of industrial wastes prompted an investigation of the chemical and mineralogical composition and properties of kaolinite, pyroxene, and electrothermic phosphoric industrial waste products. Glass and glass ceramics are produced from this industrial waste by founding the charge at a 1,320-1,450°C with a maximum temperature exposure of 1 hour. The chemical composition of the glass and glass ceramics and such process indicators and properties as the founding temperature, refractive index, density, chemical stability, crystallization range, softening point, temperature coefficient of linear expansion, and microhardness are summarized. An analysis of the physical and chemical properties of the resulting products confirms the expediency of using kaolin, pyroxene, and electrothermophosphoric slag as raw materials for making glass crystalline materials; these materials may be used as tiles and for lining mill drums operating in corrosive media. Tables 5.

### Ceramic Catalyst Carriers for Conducting Chemical Processes and Scrubbing Gas Discharges

927D0153B Moscow STEKLO I KERAMIKA  
in Russian No 1, Jan 92 pp 3-6

[Article by Ye.Ya. Medvedovskiy, A.V. Fedotov, V.P. Rudnitskaya, O.A. Sheronova, F.Ya. Kharitonov, Electric Grade Porcelain Scientific Production Association; UDC 666.77:66.093.673]

[Abstract] The effect of the shape and size of catalytic elements and catalyst carriers on the efficiency of heterogeneous catalytic reactions, especially gas scrubbing, is discussed and it is noted that ceramic catalyst carriers are especially suitable due to their high resistance to thermal shock and corrosive media, sufficient strength, the ability to operate at elevated temperatures, and the possibility of manufacturing products with diverse configurations, porosity, activity, and macro- and microstructure. Several specific types of catalyst carriers, e.g., honeycomb and porous structures, from high-alumina ceramics and cordierite, silica, and zeolite ceramics are considered and their open porosity, mean pore size, and crushing strength are summarized. Pilot batches of ceramic carriers on the basis of high alumina (with a 70-100 percent  $Al_2O_3$  concentration), cordierite, and anatase ceramics shaped as tubes, rings, cylinders, and honeycomb blocks have been successfully tested in a number of chemical processes and gas scrubbing operations at power plants. Figures 1; tables 1; references 8: 3 Russian, 5 Western.

### High-Capacity Plate Glass Furnace Operation Analysis by Physical Modeling Method

927D0153D Moscow STEKLO I KERAMIKA  
in Russian No 1, Jan 92 pp 8-10

[Article by I.M. Savina, V.P. Bespalov, L.Ya. Levitin, State Glass Scientific Research Institute; UDC 666.1.031]

[Abstract] The characteristics of mass transfer in high-capacity plate glass furnaces are discussed and the effect of mass transfer in 600-1,000 ton per day furnaces under the conditions of elevated temperatures in the bottom melt layers of the pool is investigated. To this end, the design and process parameters under which it is possible to increase the furnace output to 800 tons per day or more without worsening the founding conditions and the glass body homogenizing and fining are studied by the physical modeling method. The operating condition parameters obtained from the physical model are extended to an operating furnace by means of simulation scaling. The dependence of the flow rate at various process cycles on the furnace capacity at various maximum glass body temperatures, the charging zone length variation as a function of the furnace output, the dependence of the conditional homogenizing potential (UPG) and conditional fining potential (UPO) on the furnace output at various maximum glass body temperatures, and the dependence of the conditional fining and homogenizing potentials on the maximum glass body temperature in the pool bottom layers are plotted. An analysis of the results shows that an increase in the furnace capacity leads to a weakening of the convective flux components in the furnace; in order to maintain the founding conditions at a high level while increasing the furnace output from 600 to 1,000 tons per day, it is necessary to increase the founding pool temperature by roughly 70-80°C by utilizing the heat insulation. The model study demonstrates the advantages of simulation which makes it possible to obtain valuable data without complicated and labor-consuming experiments. Figures 4; references 4.

### Using Mathematical Model of Glass Density Prediction to Control Tank Furnace

927D0153E Moscow STEKLO I KERAMIKA  
in Russian No 1, Jan 92 pp 11-12

[Article by R.I. Makarov, I.R. Dubov, S.A. Lukashin, Vladimir Polytechnic Institute and Borskiy Glass Works; UDC 666.1.031]

[Abstract] The use of the glass density as a symptom of the glassmaking furnace performance and the correctness of the charge composition is discussed and the factors affecting the glass density—the chemical composition, thermal conditions, and charge pretreatment—are considered. To this end, production line No. 1 (LPS-5000) for making polished glass at the Borskiy Glass Works is examined in order to ascertain the extent to which the charge composition and the glassmaking

furnace operating conditions affect the density of the final glass. A mathematical model which reliably describes density by a linear regression equation is derived. The 24-hour average glass mass temperature, density, optical zebra distortions, stria index, and specific gas consumption are summarized. The resulting model is used to adjust the thermal conditions and develop a furnace process control algorithm. An increase in the bottom furnace temperature to 1,150°C along the first burner pair axis and to 1,250°C along the third pair axis makes it possible not only to stabilize the tank furnace operation but also to produce high-quality polished glass. Tables 1, references 4.

#### **Effect of Shielding Atmosphere Composition on Adhesive Properties of Soda Lime Glass**

927D0153F Moscow STEKLO I KERAMIKA  
in Russian No 1, Jan 92 pp 13-14

[Article by V.E. Solinov, T.V. Kaplina, A.V. Gorokhovskiy, NITS, Tekhstroysteklo Scientific Production Association, and Saratov Polytechnic Institute; UDC 666.11.01:532.64]

[Abstract] The task of establishing the effect of process parameters of the melt pool on the operating properties of thermally polished sheet glass is formulated and the dependence of the adhesive properties of the upper and lower surfaces of sheet glass molded at various hydrogen concentrations in the pool's shielding atmosphere and at various glass body temperatures in the production channel is examined. The adhesive properties of the glass samples taken from the glass sheet are determined by measuring the adhesion strength of the glass surface bond with the B-17 polyvinylbutyral film pursuant to GOST 9438-85. The dependence of the adhesion strength of the upper and lower soda lime glass sheet on the glass body temperature in the channel and the dependence of the adhesion strength variation coefficient of the upper and lower soda lime glass surface on the glass body temperature in the channel are plotted. The dependence of the adhesion strength and variation coefficient on the volume fraction of hydrogen and temperature is summarized; the findings indicate that an increase in the H<sub>2</sub> concentration in the shielding atmosphere increases the adhesion of the upper surface of thermally polished glass to polymers with electron-donor functional groups, making it possible to improve the properties of a number of products using sheet glass; on the other hand, an increase in the hydrogen concentration is undesirable for soda lime glass used as the matrix for making clear acrylic plastic since an increase in its surface adhesion leads to defects. Figures 2; tables 1, references 5.

#### **Absorption Spectra of Staining Dopants in Glass From Synthetic Charge**

927D0153G Moscow STEKLO I KERAMIKA  
in Russian No 1, Jan 92 pp 14-15

[Article by A.B. Atkarskaya, V.I. Borulko, Yu.I. Rastorguyev, V.S. Shashkin, Scientific Research Institute of Automotive Glass; UDC 666.22]

[Abstract] The requirements imposed on colorless and optical glass and the methods of avoiding glass contamination during its production and lowering the founding temperature and duration and, consequently, reducing the erosion of refractories by using synthetic batch are discussed and the effect of the batch type on the behavior of the five principal staining impurities—iron, copper, chromium, nickel, and cobalt—in a glass with a close to K-18 content is investigated. The synthetic batch is prepared by liquid phase hydrolysis of tetraethoxysilane by an aqueous dopant solution at pH = 7, thermal coagulation, and heat treatment. The glass transmissivity is measured by an SF-46 instrument within a 400-1,100 nm band while the specific absorption coefficients (UPP) are calculated by a known formula. Absorption spectra of Fe, Cu, Cr, Co, and Ni in glass samples are plotted. An analysis demonstrates that during the founding of alkali borosilicate glass, synthetic batch creates stronger reducing conditions than the traditional charge; the proportion of low-valence forms of Fe (II) and Cu (I) staining dopants in the glass from synthetic batch is substantially higher. Absorption by Cr, Ni, and Co does not depend on the batch production method. It is noted that more oxidizing conditions must be created for founding glass from synthetic batch; this can be accomplished by adding arsenic oxide. Figures 2; tables 1; references 5; 4 Russian, 1 Western.

#### **Investigation of Low-Temperature Ceramics Firing Process by Electron Paramagnetic Resonance and Magnetostatic Methods**

927D0153H Moscow STEKLO I KERAMIKA  
in Russian No 1, Jan 92 pp 19-22

[Article by K.A. Kuvshinova, N.Yu. Yakubovskaya, Ye.S. Grigoryan, V.M. Loginov, N.S. Yugay, Ye.P. Gorbato, L.M. Budashkina, All-Union Scientific Research Institute of Mineral Raw Materials and Gzhel Production Association; UDC 666.5.015.4]

[Abstract] The advantages of the electron paramagnetic resonance (EPR), infrared spectroscopy (IKS), nuclear  $\gamma$ -resonance (YaGR), magnetometry, and electron microscopy methods for studying the low-temperature ceramics firing process are discussed and the possibility of using electron paramagnetic resonance and magnetostatic methods for monitoring the process of first (non-glazing) roasting of the porcelain body on the basis of the Prosyanyaya deposit kaolin is investigated; the physical principles of the electron paramagnetic resonance are explained. Porcelain body samples are examined by an EP-420 radio spectrometer (Bruker) and a miniature REM-1034 spectrometer; magnetostatic studies are carried out using a Kapperbridge KLY-2 digital bridge (CzSR). The dependence of the electron paramagnetic resonance line intensity of various centers and magnetic susceptibility on the porcelain body firing temperature, the electron paramagnetic resonance spectrum of the B-center at a 20°C porcelain body temperature, the

correlation between the magnetic susceptibility and electron paramagnetic resonance line intensity of the *B*-center of lab-fired and furnace-fired samples, the intensity distribution of the electron paramagnetic resonance spectrum lines and magnetic susceptibility of samples fired in various sections of the furnace, and the oxidation and reduction area distribution in a furnace are plotted. An analysis of the findings demonstrates that electron paramagnetic resonance and magnetostatic data are highly informative and provide additional information about the firing process. These data make it possible to clarify the temperature variation ranges of the first firing at various shelves in the furnace and plot the magnetic parameter distribution charts, thus helping to identify gas condition violations and determine the heat flux direction in the furnace. The authors are grateful to G.N. Maslennikova for interest in the effort and valuable remarks. Figures 7; references 4.

#### Ceramic Sheet Molding Method by Vacuum Filtration

927D0153I Moscow STEKLO I KERAMIKA in Russian No 1, Jan 92 pp 22-24

[Article by M.K. Galperina, V.K. Kanayev, N.V. Kolyshkina, Building Ceramics Scientific Research Institute; UDC 666.3-413]

[Abstract] Methods of molding ceramic sheets by semidry compaction and slip casting onto a consumable (combustible) base and their shortcomings are discussed and a new technology of molding ceramic sheets and slabs by vacuum filtration which differs principally from the above methods in that the molding and dehydration processes are performed in a drum vacuum filter is described. The new technology is characterized by lower fuel and electric power outlays. The method amounts to slip preparation in ball mills, slip coagulation in tanks with an impeller, vacuum filtering in a drum, heating, decoration, drying, and firing. The filtering properties of the slip are examined by a submerged funnel and the slip structure is studied by the changes in its effective viscosity recorded by a Rheotest-2 viscosimeter. The dependence of the slip fluidity and sediment layer thickness on the electrolyte content, the slip structure behavior under the effect of diluting electrolytes and the M-3 binder, and the effect of the M-3 binder on the slip filtering properties are plotted and a schematic diagram of the ceramic sheet molding method is cited. The sodium silicate solution content, coagulating additive type and content, filtering duration, slip moisture content, fluidity, sediment layer thickness, and sediment moisture content are summarized. The new technology is environmentally clean. Figures 4; tables 1; references 3: 1 Russian, 2 Western.

#### Chain Structure Silicate-Based Ceramic Pigments

927D0153J Moscow STEKLO I KERAMIKA in Russian No 1, Jan 92 p 26

[Article by N.A. Sirazhiddinov, N.N. Akramova, F.I. Velikanova, L.Z. Pulatova, B.M. Akhmedov, Chemistry Institute at the Uzbek Academy of Sciences and Tashkent Scientific Research and Design Institute of Building Materials; UDC 666.622:666.3.022]

[Abstract] The declining pigment imports which limit the production of ceramic tiles with a color finish prompted attempts to develop production of ceramic pigments in Uzbekistan; to this end, the possibility of using local raw materials—wollastonite concentrate whose structure is based on chains of bound Si-O tetrahedrons forming continuous SiO<sub>2</sub> chains—which are characterized by considerable resistance at high temperatures, is examined. X-ray structural analysis of the synthesized pigments indicates that the phase composition of the roasted sinter is predominantly that of wollastonite. The synthesized pigments have good chromomorphous properties; their addition to industrial glaze in the amount of 2-7 percent makes it possible to produce a glazed surface from pale lilac to deep lilac in color; the pigment is stable to the glaze's dissolving action and to high temperatures.

#### All-Ceramic Housing Parts of High-Temperature Electric Connectors

927D0153K Moscow STEKLO I KERAMIKA in Russian No 1, Jan 92 pp 30-31

[Article by M.Yu. Khitrov, G.B. Sabun, Kazan Scientific Research Institute of Cylindrical Connectors; UDC 666.65]

[Abstract] The shortcomings of the VK 94-1 and VK 94-2 high-temperature aluminum oxide-based ceramics and electric products from them, particularly the low insulation resistance at temperatures above 500°C, are outlined and the advantages of the high-alumina (corundum) VK 100-1, VK 100-2, A-995, and stoal which contain more than 99 percent Al<sub>2</sub>O<sub>3</sub> and have virtually no vitreous phase are discussed. It is noted that electric parts and insulators made by Cannon, Amphenol, and Bendix remain serviceable at a temperature of 750°C. Consequently, attempts are made to make housing parts for temperature- and scaling-resistant electric connectors from the VK 100-2 ceramics (polikor). The manufacturing process is described and several types of ceramic connectors are shown. The microstructure of the ceramic parts is examined; the connectors are tested at a temperature of 530, 730, and 1,030°C. Test data make it possible to recommend the VK 100-2 ceramics as structural material for making high-temperature housings and bases of electric (unsealed) connectors operating at ambient temperatures of 500°C for 1,000 h, 700°C for 250 h, and 1,000°C for 3-5 h. Figures 3; references 1.

**END OF**

**FICHE**

**DATE FILMED**

19 June 1992